Histol Histopathol (2008) 23: 1025-1033

**http://www.hh.um.es**

**Histology and Histopathology**

*Cellular and Molecular Biology*

## *Review*

# Structural and functional insights into nucleocytoplasmic transport

**Martin Beck[1] and Ohad Medalia[2]**

[1]Institute of Molecular Systems Biology, The Swiss Federal Institute of Technology, Zürich, Switzerland and

[2]Department of Life Sciences, Ben Gurion University and the NIBN, Israel

**Summary.** The cell nucleus is surrounded by a double membrane system, the nuclear envelope (NE), with the outer nuclear membrane being continuous with the endoplasmic reticulum. Nuclear pore complexes (NPCs) fuse the inner and outer nuclear membranes, forming aqueous channels that allow free diffusion of small molecules but that also mediate the energy-dependent transport of large macromolecules. The NPC represents the largest known molecular complex and is composed of about 30 different proteins, termed nucleoporins (Nups). Here, we review recent studies that provide novel insight into the structural and functional organization of nucleocytoplasmic transport. In addition, prospects towards a high resolution model of the nuclear pore are discussed.

**Key words:** Cryo-electron tomography, Nuclear pore complex structure, Nucleocytoplasmic transport, Nucleoporin

### Introduction

The transport of macromolecules across the nuclear envelope is mediated by the nuclear pore complex (NPC). Over the last two decades, substantial structural and biochemical study has revealed the overall organization of this channel. Consisting of three rings, the NPC scaffold exhibits an eight-fold rotational symmetry and forms the main channel through which bidirectional transport occurs (Fig. 1A). The spoke ring complex, which forms the central channel, is flanked by the cytoplasmic and nuclear rings, on the corresponding sides of the nuclear envelope. Eight flexible filaments, thought to interact with transmitting cargo, are attached to the cytoplasmic ring (Franke et al., 1981; Pante and Aebi, 1996; Goldberg et al., 2000; Kutay and Guttinger, 2005; Cole and Scarcelli, 2006). An additional eight filaments emanating from the nuclear ring are joined to the distal ring forming the nuclear basket (Fig. 1A,B) (Ris, 1991; Goldberg and Allen, 1996). Within the center of the central channel resides an electron dense substructure, termed the central plug (Fig. 1C,D). The components comprising the different structural elements, the nucleoporins, are synthesized as soluble proteins before being incorporated into the complex. The entire NPC is believed to be anchored to the NE via three membrane proteins, i.e. Pom121, gp210 and NDC1, in vertebrates.

*Offprint requests to:* Martin Beck, Institute of Molecular Systems Biology, The Swiss Federal Institute of Technology, Wolfgang Pauli-Str. 16, CH-8093, Zürich, Switzerland. e-mail: Merin Beck (beck@imsb.biol.ethz.ch) Ohad Medalia (omedalia@bgu.ac.il)

### Three-dimensional reconstructions of NPCs

The first three-dimensional (3D) reconstruction of the NPC appeared in the early 1980's (Unwin and Milligan, 1982), when negatively-stained *Xenopus* NPCs were investigated by single particle analysis using transition electron microscopy (TEM). The subsequent development of cryo-electron microscopy (Adrian et al., 1984) facilitated reconstructions of *Xenopus* (Akey and Radermacher, 1993; Stoffler et al., 2003) and yeast nuclear pores (Yang et al., 1998). The structure of the *Dictyostelium* NPC (Beck et al., 2004) was determined following further conceptual advances, namely the application of cryo-electron tomography (cryo-ET) to intact nuclei and enabled better structural preservation than previously attained. Together with the development of a novel algorithm for structure determination (Förster et al., 2005), the first 3D reconstruction of the NPC from a frozen-hydrated specimen was obtained without the introduction of an artificial elongation along the nucleocytoplasmic axis. The appearance of such an

elongation, a consequence of non-isotropic sampling in angular space, had plagued earlier efforts (Grunewald et al., 2003). A cataloguing of human and yeast nucleoporins against the *Dictyostelium* genome suggests the NPC in all three species to present a similar protein composition (Fig. 2A), although the homologies of the *Dictyostelium* Nup sequences to their human orthologues are usually higher than to their yeast counterparts. Moreover, GFP-fusion proteins of *Dictyostelium* Nups localize to the nuclear envelope, demonstrating the reliability of the sequence alignment-based homology assignments (Fig. 2B).

The scaffold structure of the *Dictyostelium* nuclear pore spans 50 nm across the nuclear envelope, with an outer diameter of 125 nm. A limiting factor for the resolution obtainable is the structural heterogeneity of the NPC in terms of composition and dynamic movements. Indeed, plasticity of the nuclear pore was reported (Akey, 1995), while the mean residence times of nucleoporins was found to vary from seconds to hours (Rabut et al., 2004). Furthermore, nine- and ten-fold rotationally symmetric NPCs have been identified (Hinshaw and Milligan, 2003), arguing for the existence of flexible interfaces between the asymmetric units of the complex. A 3D quantification of the deviation of the asymmetric units (i.e. protomers) from their ideal positions indicated that 20% of the protomers shifted more than 5 nm from their ideal position within the spoke ring plane (Beck et al., 2007), thereby forcing the overall arrangement of the NPC to assume a slightly elliptical shape. Taking these deviations into account, the resolution of the scaffold structure, in the context of the inner and outer nuclear membranes, was improved to 5.8 nm. At such resolution, it becomes obvious that the spoke ring complex is attached to the fused nuclear membranes, while the cytoplasmic and nuclear rings present larger outer diameters, situated at both sides of the membrane curvature (Fig. 1).

Since the three NPC rings are spatially separated, different pore membrane proteins (POMs) might serve to anchor the rings at differential positions. It was demonstrated that yeast POM34, genetically linked to

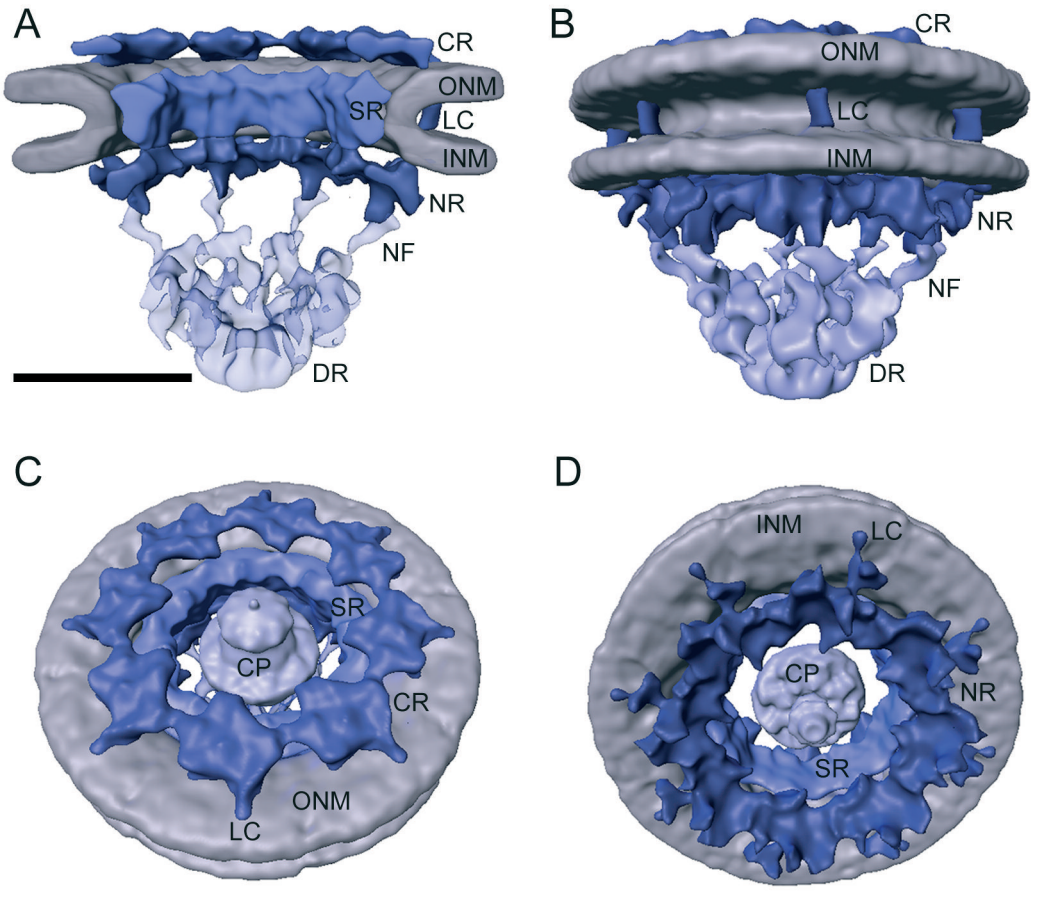


**Fig. 1.** Three-dimensionally rendered images of the Dictyostelium NPC. Elements of the scaffold structure consisting of the cytoplasmic (CR), spoke (SR) and nuclear rings (NR) as well as the lumenal connector (LC), are shown in shades of blue. The outer (ONM) and inner nuclear membrane (INM) are shown in grey. **A.** Cut-open view along the nucleocytoplasmic axis. The basket, consisting of nuclear filaments (NR) and the distal ring (DR), is shown in transparent blue (scale bar: 60 nm). The central plug has been omitted for clarity. **B.** The entire structure is shown in the same orientation as in **(A)**; the nuclear basket was rendered in bright blue. The cytoplasmic and nuclear faces of the Dictyostelium NPC are shown in **(C)** and **(D)**, respectively. The central plug (CP) is shown in bluish grey, while the nuclear basket has been omitted in **(D)** for clarity. The structural modules and their dimensions are similar to those in the vertebrate NPC. As compared to the spoke ring, the cytoplasmic and nuclear rings have larger outer diameters and are connected through the rod-shaped lumenal connector. While the spoke ring is continuous with the fused membranes, the cytoplasmic and nuclear rings are in contact with the INM and ONM, respectively, thereby forming a 'sandwich'-like structure.

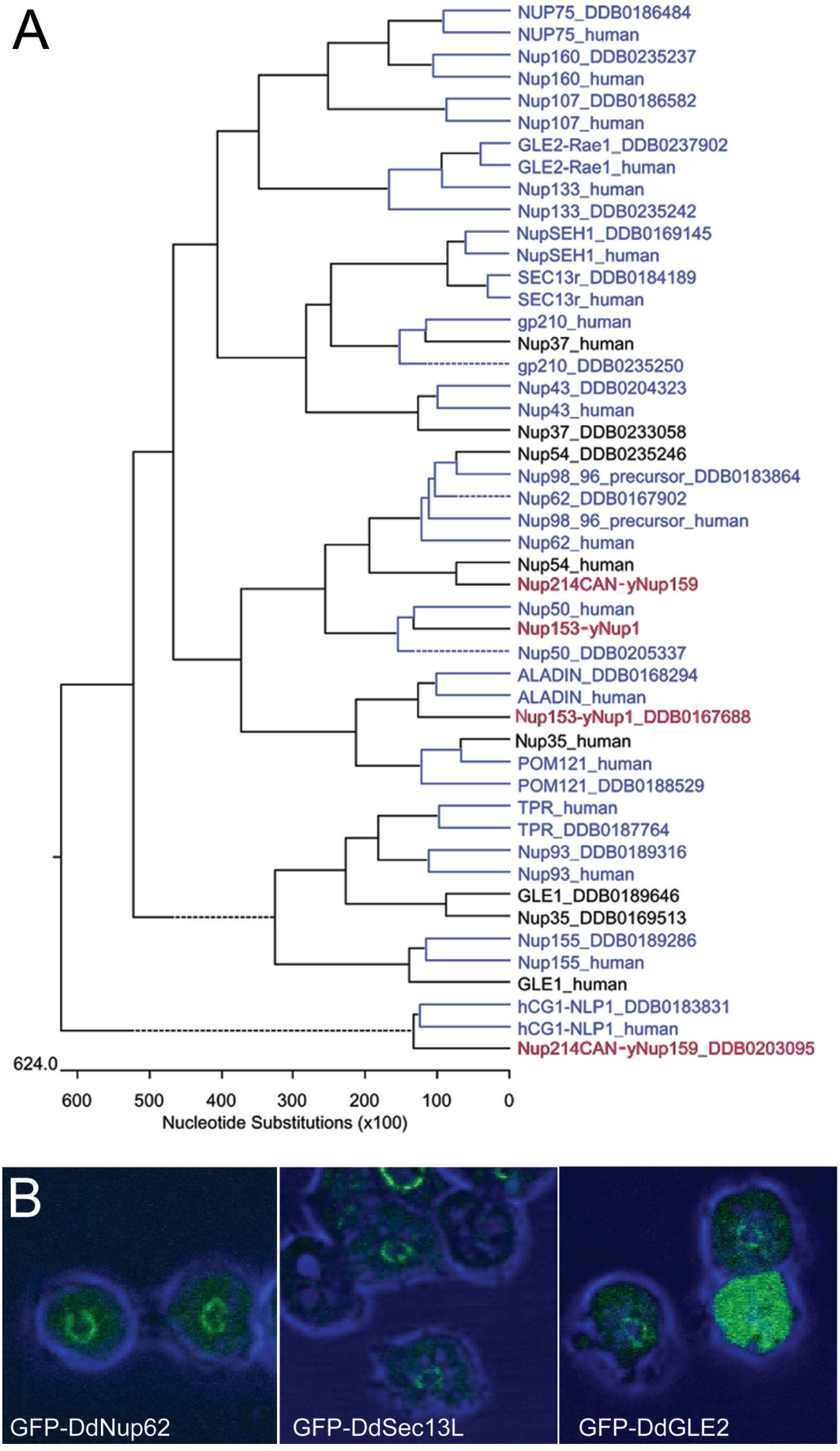


**Fig. 2.** The *Dictyostelium* nuclear pore complex (NPC). **A.** Phylogenetic tree showing nucleoporins (Nups) identified in the *Dictyostelium* genome sequence (DictyBase identification numbers are shown, nomenclature according to human orthologues). In almost all cases, the human orthologues are more closely related to the *Dictyostelium* sequences than are the yeast orthologs (except for yNup159 and yNup1, marked red). In addition, the sequence conservation between human and *Dictyostelium* orthologs is usually higher than between different *Dictyostelium* Nups, suggesting functional conservation through evolution (homologous pairs are marked blue). **B.** GFP-fusion proteins of the identified *Dictyostelium* Nups localize to the nuclear envelope.

different NPC subcomplexes, contains a lumenal loop domain and two domains facing the cytoplasmic side of the nuclear envelope (Miao et al., 2005). Therefore, POM34 might not only connect distinct sub-structures, but may also form a bridge into the lumenal space. While the electron density of the lumenal NPC component of vertebrates was described as ring-shaped (Akey, 1995), the *Dictyostelium* NPC, by contrast, has one rod-shaped lumenal element per asymmetric unit, connecting the cytoplasmic and nuclear rings (Fig. 1). This connector spans the entire lumenal space and thus defines the distance between the cytoplasmic and nuclear rings or between the inner nuclear membrane (INM) and the outer nuclear membrane (ONM), respectively. Therefore, the lumenal connectors may represent the critical element for fixing membrane curvature. The LINC-complex, formed by the SUN proteins and Nesprin, couples the INM to the ONM (Crisp et al., 2006). Recent study has shown that SUN2 is associated with nuclear pores (Liu et al., 2007). As such, one could speculate that this protein might also be part of the lumenal connector element. Interestingly, the scaffold nucleoporin, Nup133, contains an amphiphatic α-helix for sensing membrane curvature (Drin et al., 2007). Hence, Nup133 is likely to contribute to membrane anchorage, in addition to the three transmembrane nucleoporins.

Peripheral channels with a diameter of about 5 nm are formed at the interface of the fused membranes and the spoke ring complex at each asymmetric unit of the *Dictyostelium* NPC. These channels have also been described for *Xenopus* nuclear pores and their role in the facilitated diffusion of small molecules has been discussed (Stoffler et al., 2003). Nevertheless, King and co-workers demonstrated that the transport of inner nuclear membrane proteins propagates along the pore membrane domain (King et al., 2006). Consequently, the lumenal connector, together with the cytoplasmic and nuclear rings, might bring the INM and ONM into close proximity, while the spoke ring would fuse the membranes forming peripheral channels to enable the transport of INM proteins to their final destinations.

## Nucleoporins and modularity

The nuclear pore is composed of 30 different nucleoporins, most consisting of several distinct domains and present in 8-32 copies within an individual NPC. Although low resolution models of the NPC have been offered, information at the atomic resolution level is crucial to ultimately understanding the structural organization of the nuclear pore. While the basic NPC building blocks share a similar set of folding motifs (Fig. 3, lower section), a few specialized domains exhibit more unique folds (Fig. 3, upper section). The structure of the auto-proteolytic domain of Nup98, a nucleoporin involved in RNA export and encoded by two alternatively spliced mRNA transcripts, has been revealed by X-ray crystallography (Hodel et al., 2002). The C-terminal domain of Nup98 presented a novel protein fold and, therefore, represents a new class of autocatalytic proteases (Fig. 3). Since the associated peptide tail of Nup96 was co-crystallized with Nup98, this structure serves as a model for Nup98-Nup96 interaction. The C-terminal domain of the yeast Nup98 orthologue, Nup116p, has the same fold and exists in multiple conformations, as revealed by nuclear magnetic resonance (NMR) (Robinson et al., 2005). The freedom of conformational changes experienced by Nup116p was tremendously reduced upon binding to the N-terminal peptide of Nup145p, its C-terminal auto-proteolytic partner (comparable to the human Nup98-Nup96 interaction). The different conformations of Nup116p allow the protein to shuttle between multiple binding partners within the NPC. This may provide an important hint to the dynamics transpiring at the secondary and tertiary structure levels, events presumably underlying those deviations that occur within the overall assembly.

Nup358 is a multi-domain protein that fulfils several functions. The crystal structure of the SUMO-E3-ligase domain of Nup358 in complex with Ubc9, SUMO and RanGAP offered new insight into the SUMOylation mechanism employed by this protein (Reverter and Lima, 2005). The structure of the Ran-binding domain 2 of Nup358 was investigated by NMR and shown to contain a ß-barrel fold with an additional ß-strand not observed by X-ray crystallography (Geyer et al., 2005). This finding is, furthermore, in agreement with the crystal structures of the Ran-binding domain 1 of Nup358 in complex with Ran (Vetter et al., 1999) and Ran-binding protein 1 (RanBP1) in complex with Ran and RanGAP (Seewald et al., 2002). In general, Ran-binding motifs exhibit a pleckstring-homology domain fold contacting the acidic C-terminus of Ran through a patch of basic residues (Fig. 3).

Until recently, the structure of the basic building blocks of nuclear pores remained elusive. Due to the low degree of sequence conservation between nucleoporins, prediction of their folds presents a serious challenge. Two independent studies, however, have revealed the first structures of nucleoporin folds (Berke et al., 2004; Weirich et al., 2004). These are apparently common to other components of the NPC and, therefore, depict basic elements. Weirich and co-workers have shown that the N-terminal domain of Nup159, the yeast homologue of hNup214, folds into an asymmetrically arranged, seven-bladed ß-propeller (Weirich et al., 2004). Proteins of the ß-propeller family fulfil diverse cellular functions, with many serving as hub proteins, interacting with multiple partners (Fulop and Jones, 1999). Nup159, in particular, recruits the DEAD box helicase, DBP5, to the cytoplasmic face of the NPC during nuclear export. Another study demonstrated that the N-terminal domain of hNup214 folds into a ß-propeller (Napetschnig et al., 2007). Also addressing nucleoporin folds, Berke and co-workers found that the C-terminal domain of Nup133 similarly resembles a seven-bladed ß-propeller (Fig. 3) with differential surface properties that would enable this

nucleoporin to participate in multiple interactions (Berke et al., 2004). This study predicts that ß-propeller folds correspond to important basic structural elements found in one third of all nucleoporins. The authors suggest, moreover, that repetition at the tertiary structure level conceptually simplifies the assembly and disassembly of NPCs. Meanwhile, computational analysis based on sequence alignment and fold assignment suggests that the major part of 83% of the yeast NPC consists of ß-propellers, α-solenoids or FG-repeats (Devos et al., 2006), the latter being natively unfolded (Denning et al., 2003). Devos and co-workers grouped nucleoporins into three general classes, based on their structure: (i) POMs share cadherin folds and transmembrane helices, (ii) the scaffold group that contains α-solenoids, ß-propellers or both and (iii) the FG-group, presenting FG-repeat domains and coiled-coil motifs. Consequently, the scaffold structure of the NPC consists of highly abundant and evolutionary ancient alpha-only and beta-only domain folds. Since the particular arrangement of an N-terminal -propeller followed by an -solenoid is found only in nucleoporins, clathrin/adaptin complexes and coatomer protein complexes I and II, a common origin for the Nup107-160 subcomplex and vesicle coat proteins has been suggested (Devos et al., 2004). Although controversial (Antonin and Mattaj, 2005), the idea of an early membrane-curving module leading to the formation of the internal membrane systems in modern eukaryotes is certainly appealing. Interestingly, Drin and co-workers have identified a general amphiphatic a-helical motif for sensing membrane curvature, also found in the Golgi-associated protein, ArfGAP-1, as well as in Nup133 (Drin et al., 2007), a member of the Nup107-subcomplex (see below). Recently, the structure of the scaffold nucleoporin, Nic96, the yeast orthologue of Nup93, was solved by X-ray crystallography (Fig. 3). Although Nic96 is elongated and mostly -helical, it does not share the hallmark features of solenoid proteins, i.e. a regular repeat pattern that forms a spiral-shaped superhelix (Jeudy and Schwartz, 2007), and, therefore, stands in contrast to earlier structural predictions (Devos et al.,

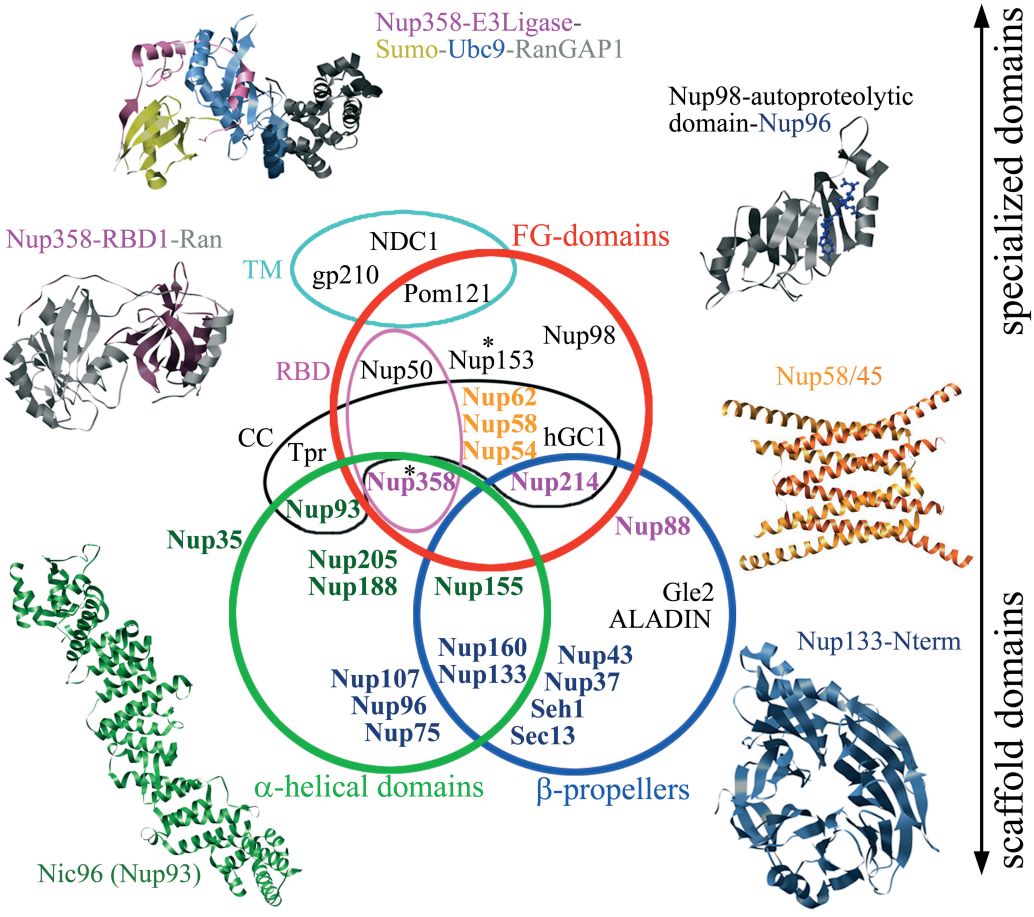


**Fig. 3.** Set graph of nucleoporins according to fold. The three circles depict the major structural motifs: α-helical domains (green), ß-propellers (blue) and FG-repeat domains (red). Coiled-coils (CC, black), Ran-binding domains (RBD, pink), transmembrane motifs (TM, cyan) and zinc fingers (asterisk) are also depicted. Scaffold motifs are shown in the lower section of the figure, which functionally-devoted motifs are presented in the upper section. Nucleoporins presumably share similar folds within known subcomplexes (in bold letters): Nup107-Nup160 (bottom, blue), Nup205-188 (middle left, green), Nup214 (middle right, pink) and Nup62 subcomplex (center, orange). The crystal structures shown are the Nup358-Ran-binding-domain in complex with Ran, the Nup358-E3-Ligase-domain in complex with SUMO, Ubc9 and RanGAP, the Nup98 auto-proteolytic domain in complex with a Nup96 peptide, the N-terminal domain of Nup133, the alpha-helical region of Nup58 associated with its splice variant Nup45, and Nic96, the yeast orthologue of Nup93 (Vetter et al., 1999; Hodel et al., 2002; Berke et al., 2004; Reverter and Lima, 2005; Jeudy and Schwartz, 2007; Melcak et al., 2007).

2006).

Finally, nucleoporins within known subcomplexes, such as the Nup107-160, the Nup205, the Nup214-88 and the Nup62 subcomplexes, share similar folding motifs (Fig. 3) and presumably form the individual NPC substructures. The position of many nucleoporins was roughly mapped onto the overall assembly and most showed symmetrical localization, relative to the NE (Rout et al., 2000). However, most of the studies relying on immunocytochemistry were performed using gold-labeled secondary antibodies, a tool that imparts a precision of ~16 nm (Baschong and Wrigley, 1990). This strategy is sufficient to characterize elongated structures but when applied to scaffold nucleoporins, may introduce an artificial symmetry around the center of the spoke ring complex, since the gold clusters would localize along a circular perimeter around the epitope. Nevertheless, while some subcomplexes contain more scaffold motifs and presumably localize to the core structure, others contain more functionally devoted folds that would presumably localize to the NPC periphery (Devos et al., 2006).

The Nup107-160 subcomplex (Fig. 3, blue) consists exclusively of scaffold motifs, namely α-only domains and ß-propellers. Moreover, its components show long mean residence times at the NPC (Rabut et al., 2004). Biochemically, the Nup107-160 subcomplex is the best-characterized subcomplex of the NPC (Boehmer et al., 2003; Harel et al., 2003; Walther et al., 2003). The yeast homologue, i.e. the Nup84p subcomplex, can be reconstituted into an elongated structure of ~40 nm in vitro (Lutzmann et al., 2002). Since the Nup107-160 subcomplex was shown to be a key component of the NPC, one can speculate that it is part of the spoke ring complex. Except for Nup160, all components of the Nup107-160 subcomplex are present at a relative

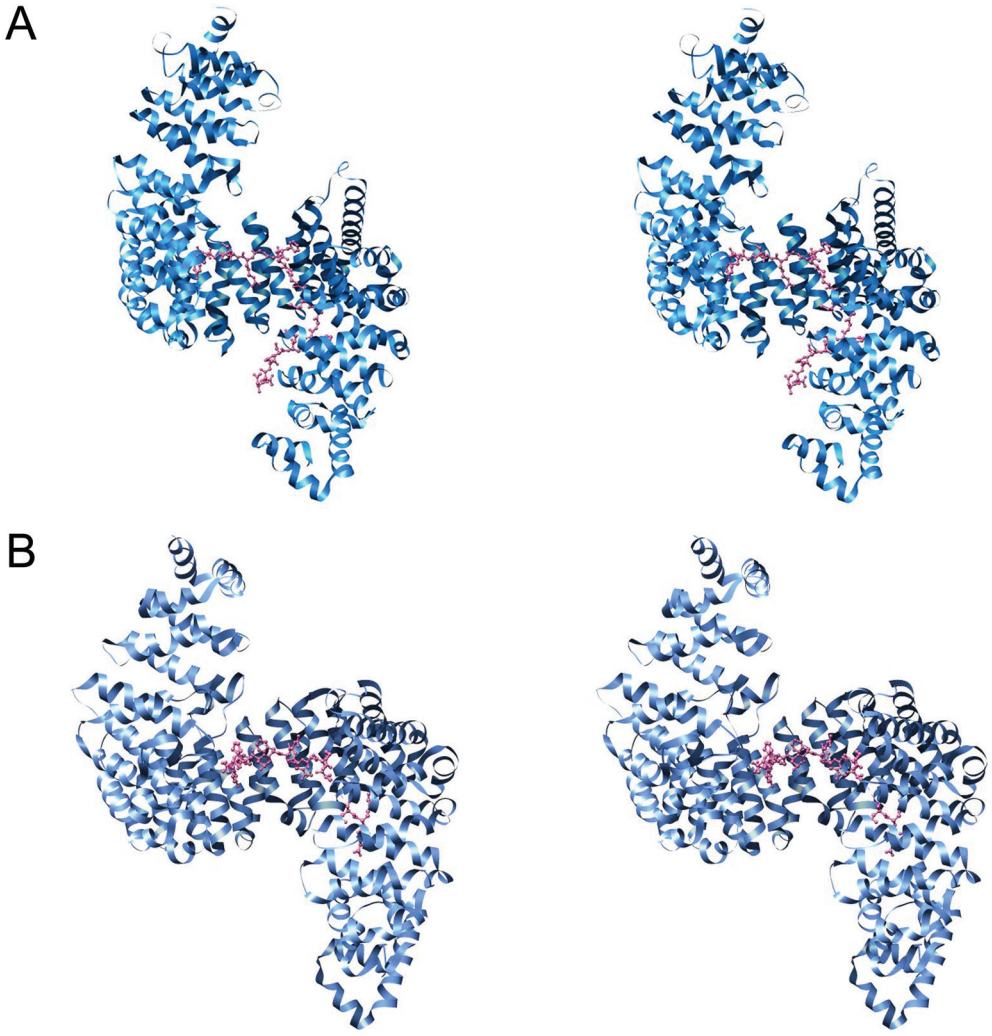


**Fig. 4.** Signal recognition by nucleocytoplasmic transport receptors. Stereo-view of 2 in complex with **(A)** M9 NLS (Lee et al., 2006) or **(B)** the NLS of the heterogeneous nuclear ribonucleoprotein M (Cansizoglu et al., 2007).

abundance of at least 2 per asymmetric unit (Cronshaw et al., 2002). The electron density of the spoke ring consists of two half rings, separated by a region of lower electron optical density (Beck et al., 2007). Consequently, the major building block of the spoke ring might contain two copies of the Nup107-160 subcomplex per asymmetric unit. The components of the cytoplasmic and nuclear rings are, however, difficult to predict at this time.

The Nup205 subcomplex (Fig. 3, green) consists mainly of scaffold motifs as well as a few additional domains. In terms of mean residence times, Nup205 subcomplex members have been partially classified into the scaffold and adaptor groups (Rabut et al., 2004). Members of the Nup214-88 subcomplex (Fig. 3, purple) contain only few scaffold domains, although various interaction motifs, such as FG-repeats, Ran-binding domains, zinc fingers and others, are present. The Nup62 subcomplex (Fig. 3, orange) is mainly composed of dynamic motifs such as coiled-coils and FG-repeats. One subcomplex member, Nup58, forms tetramers together with its splice variant, Nup45, comprising two anti-parallel α-helical hairpin dimers (Melcak et al., 2007). Melcak and co-workers have suggested that this module can adjust the diameter of the central transport channel by circumferential sliding. Interestingly, changes in NPC diameter have been detected by cryo-EM (Beck et al., 2007) and in several studies utilizing atomic force microscopy (see Lim and Fahrenkrog, 2006, for review).

## Nuclear import pathways and importin structure

In contrast to the mostly stationary nucleoporins, an additional set of soluble proteins contributes to nuclear transport. Although small ions and molecules can traverse the NPC by simple diffusion, most cargo carries specific nuclear localization signals (NLSs) or nuclear export signals (NESs), recognized by a set of transport receptors that facilitate cargo passage through the NPC. Such receptors, referred to as importins and exportins (or karyopherins), chaperone cargo during transport through the NPC by means of hydrophobic interactions with phenylalanine-and glycine-rich nucleoporin domains (FG repeats) lining the main channel. While import complexes are disassembled on the nuclear face of the NPC upon binding of RanGTP to importins, export complexes are usually escorted by RanGTP and disassembled at Ran-binding domains at the cytoplasmic side of the NPC, upon stimulation by RanGAP.

Different nuclear import pathways rely on diverse transport receptors (Gorlich and Kutay, 1999; Fahrenkrog and Aebi, 2003; Stewart, 2007), thus allowing specific substrate recognition. Here, we focus on recent advances in the structure of importins; for review of export complexes, see (Kutay and Guttinger, 2005; Cole and Scarcelli, 2006). The classical NLS that directs a broad range of cargoes (Conti et al., 1998). The NLS comes in two flavors: A short basic sequence, exemplified by that found in the SV40 large T-antigen, and a bipartite basic sequence, as found in nucleoplasmin. However, other proteins imorted into the nucleus may directly bind variants of importin ß (Conti and Izaurralde, 2001; Chook and Blobel, 2001). Following passage through the central channel, the imported cargo is released into the nucleus upon binding of RanGTP, which its high affinity for importin ß (Chook and Blobel, 2001; Lee et al., 2005).

In contrast to the relatively conserved classical NLS, other NLS sequences present considerable diversity. Accordingly, three importin ß1 variants recognizing such NLSs display significant sequence variability and structurally, present different substrate binding sites. The import of many RNA processing proteins involves direct binding of importin ß2 to the M9 NLS, a 38 amino acid transport signal found in hnRNP A1 (Fig. 4A, Pollard et al., 1996; Bonifaci et al., 1997). Indeed, several of these non-classical NLSs have been characterized by biochemical and structural approaches (Lee et al., 2006; Cansizoglu et al., 2007). Such NLSs contain a C-terminal R/H/Kx(2-5)PY motif, where x(2-5) represents a 2-5 amino acid stretch of any sequence, while the N-terminal residue is either hydrophobic or basic in nature (Fig. 4B). These 20-30 residue long sequences are structurally disordered. The non-classical NLS is oriented in an anti-parallel extended conformation, perpendicular to the α-heical HEAT repeats of importin ß2 (Cansizoglu et al., 2007). The diversity of nuclear localization signals thus emphasizes the complexity of nuclear import and the variability of signals involved in nuclear transport. Nonetheless, while NLSs that bind importin ßs vary in sequence, many share similar conformations when complexed with their import receptor, exemplifying how transport receptors might have evolved and how the specificity of various transport pathways is achieved.

## Outlook

The NPC include eight asymmetric units that form ring structures and depict the highest level in modularity hierarchy. Each asymmetric unit consist of subcomplexes that may be present in more than one copy. Different nucleoporins, however, contain domains with common folds, thereby reducing the complexity of the structure. The modularity concept (Berke et al., 2004; Schwartz, 2005) is the key to understanding how such a huge, yet intricate structure as the nuclear pore has evolved and might simplify future structural investigations aimed towards obtaining an atomic resolution model. While cryo-electron tomography represents an excellent tool for the structural analysis of functional systems, the resolution of the overall assembly is not likely to exceed 2-3 nm in the near future, due to technical limitations. The localization of specific proteins within the NPC will, therefore, require further development of gold-labelling methodology, such as the direct conjugation of gold nanoparticles to Nups in combination with 3D-EM approaches. Consequently,

single particle cryo-EM of defined subcomplexes might well serve to close the resolution gap to X-ray and NMR investigations. Atomic resolution structures could then be fitted into 3D maps of subcomplexes that would then be assigned into the overall structure.

*Acknowledgements.* MB was supported by a long-term fellowship from the European Molecular Biology Organization (EMBO) and a Marie Curie fellowship from the European Commission. O.M. is supported by the Israel Science Foundation (grant 794/06). We thank Dr. W. Baumeister for fruitful discussions and support and Drs. K. Knauth and J. Eichler for critical reading of the manuscript.

## References

Adrian M., Dubochet J., Lepault J. and McDowall A.W. (1984). Cryo-electron microscopy of viruses. Nature 308, 32-36.

Akey C.W. (1995). Structural plasticity of the nuclear pore complex. J. Mol. Biol. 248, 273-293.

Akey C.W. and Radermacher M. (1993). Architecture of the *Xenopus* nuclear pore complex revealed by three-dimensional cryo-electron microscopy. J. Cell Biol. 122, 1-19.

Antonin W. and Mattaj I.W. (2005). Nuclear pore complexes: round the bend? Nat. Cell Biol. 7, 10-12.

Baschong W. and Wrigley N.G. (1990). Small colloidal gold conjugated to Fab fragments or to immunoglobulin G as high-resolution labels for electron microscopy: a technical overview. J. Electron Microsc. Tech. 14, 313-323.

Beck M., Forster F., Ecke M., Plitzko J.M., Melchior F., Gerisch G., Baumeister W. and Medalia O. (2004). Nuclear pore complex structure and dynamics revealed by cryoelectron tomography. Science 306, 1387-1390.

Beck M., Lucic V., Forster F., Baumeister W. and Medalia O. (2007). Snapshots of nuclear pore complexes in action captured by cryo-electron tomography. Nature 449, 611-615.

Berke I.C., Boehmer T., Blobel G. and Schwartz T.U. (2004). Structural and functional analysis of Nup133 domains reveals modular building blocks of the nuclear pore complex. J. Cell Biol. 167, 591-597.

Boehmer T., Enninga J., Dales S., Blobel G. and Zhong H. (2003). Depletion of a single nucleoporin, Nup107, prevents the assembly of a subset of nucleoporins into the nuclear pore complex. Proc. Natl. Acad. Sci. USA 100, 981-985.

Bonifaci N., Moroianu J., Radu A. and Blobel G. (1997). Karyopherin beta2 mediates nuclear import of a mRNA binding protein. Proc. Natl. Acad. Sci. USA 94, 5055-5060.

Cansizoglu A.E., Lee B.J., Zhang Z.C., Fontoura B.M. and Chook Y.M. (2007). Structure-based design of a pathway-specific nuclear import inhibitor. Nat. Struct. Mol. Biol. 14, 452-454.

Chook Y.M. and Blobel G. (2001). Karyopherins and nuclear import. Curr. Opin. Struct. Biol. 11, 703-715.

Cole C.N. and Scarcelli J.J. (2006). Transport of messenger RNA from the nucleus to the cytoplasm. Curr Opin. Cell Biol. 18, 299-306.

Conti E. and Izaurralde E. (2001). Nucleocytoplasmic transport enters the atomic age. Curr. Opin. Cell Biol. 13, 310-319.

Conti E., Uy M., Leighton L., Blobel G. and Kuriyan J. (1998). Crystallographic analysis of the recognition of a nuclear localization signal by the nuclear import factor karyopherin alpha. Cell 94, 193-204.

Crisp M., Liu Q., Roux K., Rattner J.B., Shanahan C., Burke B., Stahl P.D. and Hodzic D. (2006). Coupling of the nucleus and cytoplasm: role of the LINC complex. J. Cell Biol. 172, 41-53.

Cronshaw J.M., Krutchinsky A.N., Zhang W., Chait B.T. and Matunis M.J. (2002). Proteomic analysis of the mammalian nuclear pore complex. J. Cell Biol. 158, 915-927.

Denning D.P., Patel S.S., Uversky V., Fink A.L. and Rexach M. (2003). Disorder in the nuclear pore complex: the FG repeat regions of nucleoporins are natively unfolded. Proc. Natl. Acad. Sci. USA 100, 2450-2455.

Devos D., Dokudovskaya S., Alber F., Williams R., Chait B.T., Sali A. and Rout M.P. (2004). Components of coated vesicles and nuclear pore complexes share a common molecular architecture. PLoS Biol 2, e380.

Devos D., Dokudovskaya S., Williams R., Alber F., Eswar N., Chait B.T., Rout M.P. and Sali A. (2006). Simple fold composition and modular architecture of the nuclear pore complex. Proc. Natl. Acad. Sci. USA 103, 2172-2177.

Drin G., Casella J.F., Gautier R., Boehmer T., Schwartz T.U. and Antonny B. (2007). A general amphipathic alpha-helical motif for sensing membrane curvature. Nat. Struct. Mol. Biol. 14, 138-146.

Fahrenkrog B. and Aebi U. (2003). The nuclear pore complex: nucleocytoplasmic transport and beyond. Nat. Rev. Mol. Cell Biol. 4, 757-766.

Förster F., Medalia O., Zauberman N., Baumeister W. and Fass D. (2005). Retrovirus envelope protein complex structure in situ studied by cryo-electron tomography. Proc. Natl. Acad. Sci. USA 102, 4729-4734.

Franke W.W., Scheer U., Krohne G. and Jarasch E.D. (1981). The nuclear-envelope and the architecture of the nuclear periphery. J. Cell Biol. 91, S39-S50.

Fulop V. and Jones D.T. (1999). Beta propellers: structural rigidity and functional diversity. Curr. Opin. Struct. Biol. 9, 715-721.

Geyer J.P., Doker R., Kremer W., Zhao X., Kuhlmann J. and Kalbitzer H.R. (2005). Solution structure of the Ran-binding domain 2 of RanBP2 and its interaction with the C terminus of Ran. J. Mol. Biol. 348, 711-725.

Goldberg M.W. and Allen T.D. (1996). The nuclear pore complex and lamina: three-dimensional structures and interactions determined by field emission in-lens scanning electron microscopy. J. Mol. Biol. 257, 848-865.

Goldberg M.W., Rutherford S.A., Hughes M., Cotter L.A., Bagley S., Kiseleva E., Allen T.D. and Clarke P.R. (2000). Ran alters nuclear pore complex conformation. J. Mol. Biol. 300, 519-529.

Gorlich D. and Kutay U. (1999). Transport between the cell nucleus and the cytoplasm. Annu. Rev. Cell. Dev Biol. 15, 607-660.

Grunewald K., Medalia O., Gross A., Steven A.C. and Baumeister W. (2003). Prospects of electron cryotomography to visualize macromolecular complexes inside cellular compartments: implications of crowding. Biophys. Chem. 100, 577-591.

Harel A., Orjalo A.V., Vincent T., Lachish-Zalait A., Vasu S., Shah S., Zimmerman E., Elbaum M. and Forbes D.J. (2003). Removal of a single pore subcomplex results in vertebrate nuclei devoid of nuclear pores. Mol. Cell 11, 853-864.

Hinshaw J.E. and Milligan R.A. (2003). Nuclear pore complexes exceeding eightfold rotational symmetry. J. Struct. Biol. 141, 259-268.

Hodel A.E., Hodel M.R., Griffis E.R., Hennig K.A., Ratner G.A., Xu S. and Powers M.A. (2002). The three-dimensional structure of the

autoproteolytic, nuclear pore-targeting domain of the human nucleoporin Nup98. Mol. Cell 10, 347-358.

Jeudy S. and Schwartz T.U. (2007). Crystal structure of nucleoporin Nic96 reveals a novel, intricate helical domain architecture. J. Biol. Chem. 282, 34904-34912

King M.C., Lusk C.P. and Blobel G. (2006). Karyopherin-mediated import of integral inner nuclear membrane proteins. Nature 442, 1003-1007.

Kutay U. and Guttinger S. (2005). Leucine-rich nuclear-export signals: born to be weak. Trends Cell Biol. 15, 121-124.

Lee B.J., Cansizoglu A.E., Suel K.E., Louis T.H., Zhang, Z. and Chook Y.M. (2006). Rules for nuclear localization sequence recognition by karyopherin beta 2. Cell 126, 543-558.

Lee S.J., Matsuura Y., Liu S.M. and Stewart M. (2005). Structural basis for nuclear import complex dissociation by RanGTP. Nature 435, 693-696.

Lim R.Y. and Fahrenkrog B. (2006). The nuclear pore complex up close. Curr. Opin. Cell Biol. 18, 342-347.

Liu Q., Pante N., Misteli T., Elsagga M., Crisp M., Hodzic D., Burke B. and Roux K.J. (2007). Functional association of Sun1 with nuclear pore complexes. J. Cell Biol. 178, 785-798.

Lutzmann M., Kunze R., Buerer A., Aebi U. and Hurt E. (2002). Modular self-assembly of a Y-shaped multiprotein complex from seven nucleoporins. EMBO J. 21, 387-397.

Melcak I., Hoelz A. and Blobel G. (2007). Structure of Nup58/45 suggests flexible nuclear pore diameter by intermolecular sliding. Science 315, 1729-1732.

Miao M., Ryan K.J. and Wente S.R. (2005). The integral membrane protein Pom34p functionally links nucleoporin subcomplexes. Genetics 172, 1441-1457.

Napetschnig J., Blobel G. and Hoelz A. (2007). Crystal structure of the N-terminal domain of the human protooncogene Nup214/CAN. Proc. Natl. Acad. Sci. USA 104, 1783-1788.

Pante N. and Aebi U. (1996). Sequential binding of import ligands to distinct nucleopore regions during their nuclear import. Science 273, 1729-1732.

Pollard V.W., Michael W.M., Nakielny S., Siomi M.C. Wang F. and Dreyfuss G. (1996). A novel receptor-mediated nuclear protein import pathway. Cell 86, 985-994.

Rabut G., Doye V. and Ellenberg J. (2004). Mapping the dynamic organization of the nuclear pore complex inside single living cells. Nat. Cell Biol. 6, 1114-U1127.

Reverter D. and Lima C.D. (2005). Insights into E3 ligase activity revealed by a SUMO-RanGAP1-Ubc9-Nup358 complex. Nature 435, 687-692.

Ris H. (1991). The three dimensional structure of the nuclear pore complex as seen by high voltage electron microscopy and high resolution low voltage scanning electron microscopy. EMSA Bull 21, 54-56.

Robinson M.A., Park S., Sun Z.Y., Silver P.A., Wagner G. and Hogle J.M. (2005). Multiple conformations in the ligand-binding site of the yeast nuclear pore-targeting domain of Nup116p. J. Biol. Chem. 280, 35723-35732.

Rout M.P., Aitchison J.D., Suprapto A., Hjertaas K., Zhao Y. and Chait B.T. (2000). The yeast nuclear pore complex: composition, architecture, and transport mechanism. J. Cell Biol. 148, 635-651.

Schwartz T.U. (2005). Modularity within the architecture of the nuclear pore complex. Curr. Opin. Struct. Biol. 15, 221-226.

Seewald M.J., Korner C., Wittinghofer A. and Vetter I.R. (2002). RanGAP mediates GTP hydrolysis without an arginine finger. Nature 415, 662-666.

Stewart M. (2007). Molecular mechanism of the nuclear protein import cycle. Nat. Rev. Mol. Cell. Biol. 8, 195-208.

Stoffler D., Feja B., Fahrenkrog B., Walz J., Typke D. and Aebi U. (2003). Cryo-electron tomography provides novel insights into nuclear pore architecture: implications for nucleocytoplasmic transport. J. Mol. Biol. 328, 119-130.

Unwin P.N. and Milligan R.A. (1982). A large particle associated with the perimeter of the nuclear pore complex. J. Cell Biol. 93, 63-75.

Vetter I.R., Nowak C., Nishimoto T., Kuhlmann J. and Wittinghofer A. (1999). Structure of a Ran-binding domain complexed with Ran bound to a GTP analogue: implications for nuclear transport. Nature 398, 39-46.

Walther T.C., Alves A., Pickersgill H., Loiodice I., Hetzer M., Galy V., Hulsmann B.B., Kocher T., Wilm M. and Allen T. (2003). The conserved Nup107-160 complex is critical for nuclear pore complex assembly. Cell 113, 195-206.

Weirich C.S., Erzberger J.P., Berger J.M. and Weis K. (2004). The N-terminal domain of Nup159 forms a beta-propeller that functions in mRNA export by tethering the helicase Dbp5 to the nuclear pore. Mol. Cell 16, 749-760.

Yang Q., Rout M.P. and Akey C.W. (1998). Three-dimensional architecture of the isolated yeast nuclear pore complex: functional and evolutionary implications. Mol. Cell 1, 223-234.

Accepted February 20, 2008